View metadata, citation and similar papers at core.ac.uk
brought to you by CORE
provided by NASA Technical Reports Server

INTERPRETING THE SOLAR WIND IONIZATION STATE

Stanley P. Owocki
Harvard-Smithsonian Center for Astrophysics
60 Garden St.
Cambridge, MA 02138

ABSTRACT

The ionization state of the solar coronal expansion is frozen within a few solar radii of the solar photosphere, and spacecraft measurements of the solar wind heavy ion charge state can therefore yield information about coronal conditions (e.g. electron temperature). Previous interpretations of the frozen-in ionization state have always assumed that in the coronal freezing-in region, 1. all heavy ions flow at the same bulk speed as protons, 2. the electron velocity distribution function is Maxwellian, and 3. conditions vary in space but not in time. In this paper, we examine the consequences of relaxing these assumptions for the interpretation of solar wind charge state measurements. We find that: 1. The temperature inferred by traditional interpretation of the interplanetary ionization state will overestimate (underestimate) the actual coronal electron temperature if higher ion charge stages flow systematically faster (slower) than lower stages at the coronal freezing radius. 2. Temperatures inferred from relative abundance measurements of ion-charge-stages (e.g. O^{+6}) with high ionization potentials moderately overestimate the actual coronal electron temperature if the high-energy tail of the coronal electron velocity distribution is enhanced relative to a Maxwellian distribution. 3. The propagation of a disturbance, e.g. a shock wave, through the corona can strongly affect the frozen-in charge state, but only over a time (a few times ten minutes) corresponding to the coronal transit time for the disturbance.

1. Introduction

The inferred degree of ionization of a gas is often used in astrophysics as a diagnostic of the gas temperature. For example, the solar-coronal ionization balance between collisional ionization and radiative and dielectronic recombination is very sensitive to the local electron temperature, but the balance is insensitive to electron density because each competing rate is proportional to the number density of electrons; information on the ionization state of the corona can thus be used to infer the electron temperature there (Billings 1966). On the other hand, as ions flow out of the corona and into the solar wind, the electron density sharply decreases so that solar wind ions hardly ever encounter an electron; the solar wind ionization balance is therefore not very sensitive to local conditions, but is "frozen" in the high-density corona within a few solar radii of the solar photosphere (Hundhausen et al. 1968a,b). Measurements of the solar wind ionization state can thus be used as a diagnostic

of the temperature in the regions of the solar corona from which the gas originates (Bame et al. 1974; Ogilvie and Vogt 1980).

In this paper, we shall first review the basic "freezing-in" theory for the solar wind ionization state (section 2). We shall then discuss several modifications of this theory which must be made when certain of its simplifying assumptions about conditions in the coronal expansion are relaxed (sections 3-5). Specifically, we shall examine the effect of unequal heavy-ion flow speeds in the corona (section 3), the effect of a non-Maxwellian coronal electron velocity distribution (section 4), and the effect of intrinsic time-variations in coronal conditions (section 5). Throughout this discussion we shall emphasize the relevance of such coronal effects to the interpretation of interplanetary charge-state measurements, but, in order to concentrate study on these effects, we shall not discuss the measurements themselves, their uncertainties, or uncertainties in assumed atomic rates.

2. The Ionization State from Simple Coronal Ion Outflows

Consider a (potentially) time-dependent coronal ion outflow in which the various ionization stages i of a given element s of atomic number Z are constantly undergoing ionization and recombination through interactions with electrons e. We write the conservation equation for each ionization stage (i=1 to Z) as,

$$\frac{\partial n_i}{\partial t}+\nabla\cdot(n_i u_i) = n_e(n_{i-1}C_{i-1}-n_i(C_i+R_i)+n_{i+1}R_{i+1}) \quad , \tag{1}$$

where n and u refer to particle number density and bulk flow velocity, and C_i and R_i refer to the ionization and recombination coefficients (cm^3/sec) for rates out of the ith ionization stage. We include here both dielectronic and radiative recombination (Burgess 1965; Tucker and Gould 1966), as well as auto- and collisional ionization (Seaton 1964; Lotz 1967), but we neglect coronal photoionization (see e.g. Billings 1966). Each rate coefficient can be written in the form $\langle\sigma v\rangle$, where σ is the cross section, v is the electron speed, and the angle brackets denote an average over the electron velocity distribution. If $n_e<10^9 cm^{-3}$, a condition valid throughout the corona and solar wind, the cross section σ is not a strong function of density (Jordan 1969), and so, if electron-electron collisions are sufficient to establish a Maxwellian distribution, then the rates $\langle\sigma v\rangle$ vary only with electron temperature; $R_i=R_i(T_e)$, $C_i=C_i(T_e)$.

Let us first examine the case in which the coronal electron velocity distribution is locally Maxwellian and the coronal outflow is steady ($\partial n_i/\partial t=0$). At the base of such a flow, the electron density n_e is relatively high while the ion velocities u_i are very small. This means that each individual rate term on

the right-hand-side of (1) has an absolute value that is much greater than the flow-divergence term described by the left-hand-side. Hence the two sides can only balance if competing rate terms approximately cancel. We therefore conclude that the ionization state of the lower solar corona is fixed by the ionization equilibrium condition,

$$\frac{n_i}{n_{i+1}} = \frac{R_{i+1}(T_e)}{C_i(T_e)} \quad , \tag{2}$$

which implies that the degree of ionization at the coronal base depends only on the local electron temperature T_e.

As ions accelerate outward from the coronal base, the local electron density rapidly decreases. In the limit of vanishing electron density at large heliocentric radii in the solar wind, each of the rate terms on the right-hand-side of (1) must individually approach zero, implying that the divergence term must also vanish, $\nabla\cdot(n_i u_i) \rightarrow 0$. We therefore find that the ionization state of the solar wind is fixed by the frozen-ion-flux condition,

$$\frac{n_i u_i}{n_{i+1} u_{i+1}} = \text{constant} \quad , \tag{3}$$

and thus is independent of local electron temperature in the wind. (Here we have assumed that different ionization stages have the same flow-tube areas, but not necessarily the same flow speeds.) Note that the ionization equilibrium conditions (2) for the solar corona fix the relative number of the ion charge stages, while the freezing conditions (3) for the solar wind fix the relative fluxes of these stages. For the remaining discussion in this section, we will assume that all ion-charge-stages flow at the same speed ($u_i = u$), in which case the distinction between relative number and relative flux becomes irrelevant. This distinction will be important, however, for understanding the effect of unequal ion flow speeds (see section 3).

This freezing of the relative charge-stage abundances occurs at the transition between dominance of the ionization/recombination processes in the low corona to dominance of flow-divergence effects in the solar wind. This transition takes place when the ionization/recombination exchange time, $\tau_{i<\rightarrow i+1} \equiv 1/n_e(R_{i+1}+C_i)$, becomes greater than the expansion time, $\tau_{exp} \equiv H/u_i$, in which the ions flow through a density scale height $H \equiv n_e/(dn_e/dr)$. Figures 1, which are adapted from Hundhausen et al. (1968a,b), illustrate this for the ionization balances among the dominant charge-stages of oxygen in a typical steady-state, spherically-symmetric coronal expansion model. In this model the electron distribution is Maxwellian, the electron temperature declines outward, and all oxygen charge-stages flow at the proton speed. Figure 1a shows how the sharp outward decline in electron density results in a rapid increase of the ion exchange time (solid curves), whereas the expansion time (dashed curves) remains

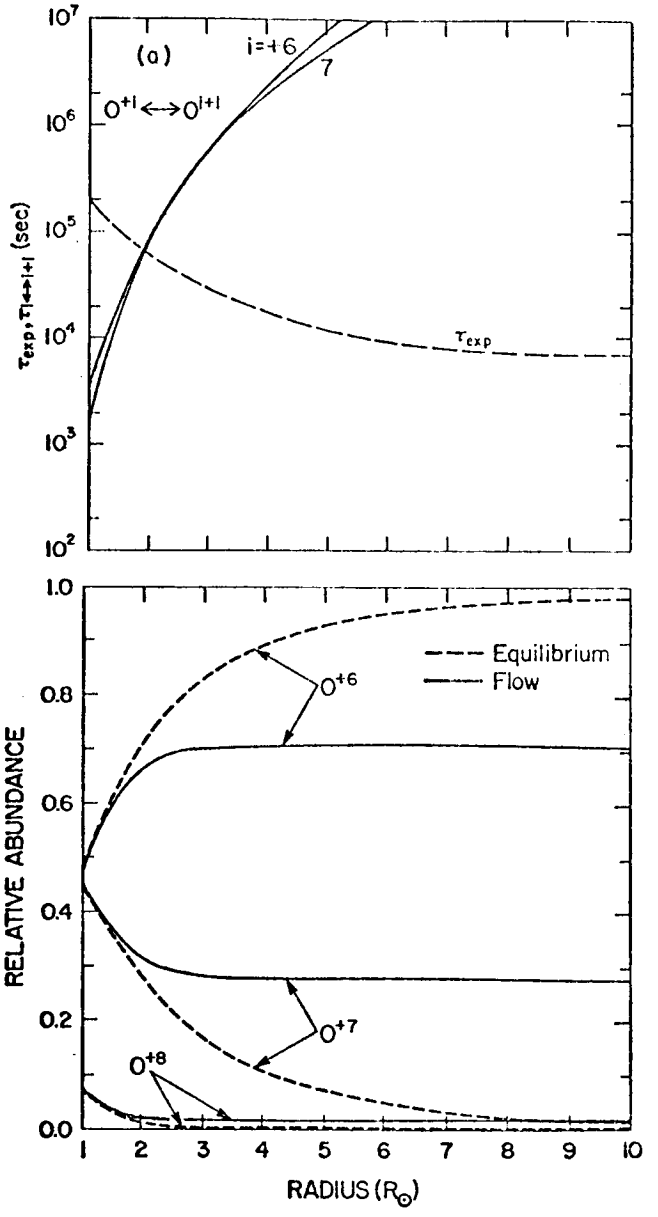

Figure 1: a. Radial variation of ion exchange time (solid curves) and ion expansion time (dashed curves) for spherically-symmetric model where all heavy ion charge-stages are assumed to flow at the proton speed. The intersection between the exchange and expansion times determine the freezing radius r_f for the given exchange.

b. Corresponding radial evolution of oxygen charge-stage abundance fractions in the flow (solid) compared with fractions that would exist in static ionization equilibrium (dashed).

relatively constant. Figure 1b compares the corresponding radial evolution of charge-stage fractions in the flow (solid) with the fractions that would exist in static ionization equilibrium (dashed). The flow-fractions initially evolve in conjunction with the equilibrium fractions (which show a shift to lower charge stages that reflects the outward decline in electron temperature); but beyond a "freezing radius" r_f (defined by $\tau_{exp}(r_f) \equiv \tau_{i<\rightarrow i+1}(r_f)$) these flow fractions "freeze" to constant values. From numerical parameter studies (Owocki 1982; Owocki et al. 1983), it is found that the frozen-in fractions often closely approximate the equilibrium fractions at the freezing radius r_f. Since the ionization equilibrium fractions depend only on local electron temperature, we conclude that measured ion fractions at large distances from the sun (e.g. at 1 a.u.) can be used to infer the electron temperature at a specific coronal freezing radius r_f.

The exact location of this freezing radius depends on the atomic properties of the ions as well as on the details of the coronal expansion. Assuming the ions flow at the proton speed, we obtain from the equation of mass continuity and from the requirement $\tau_{i<\rightarrow i+1}(r_f) = \tau_{exp}(r_f)$, an estimate of the freezing density $n_f \equiv n_e(r_f)$,

$$n_f = \left[\frac{n_E u_E \, (A_E/A_f)}{H \, (R_{i+1} + C_i)} \right]^{1/2} , \qquad (4)$$

where $n_E u_E$ is the particle flux at 1 a.u., and A_E/A_f is the ratio of flow tube areas between 1 a.u. and r_f. For spherically-symmetric outflow with a interplanetary mass flux, $n_E u_E = 3 \times 10^8 cm^{-2} s^{-1}$ (Feldman et al. 1977), we then find $n_f = 2 \times 10^7 cm^{-3}$ for the exchange among the dominant charge stages of oxygen $O^{+6} <\rightarrow O^{+7}$, while for the intrinsically faster iron exchange, $Fe^{+11} <\rightarrow Fe^{+12}$, the freezing density is much lower, $n_f = 10^6 cm^{-3}$. Using a typical "quiet" coronal density model (e.g., Newkirk 1968; Saito 1970), we obtain a freezing radius $r_f = 1.5 R_\odot$ for oxygen, and $r_f = 3.5 R_\odot$ for the iron exchange. Because of the large variation in rates for different charge-stages of iron, other iron exchanges freeze overd a range of heights from $r_f = 3$ to $5 R_\odot$ (Bame et al. 1974). Such "differential freezing" of the various ionization stages within a given species can give rise to some subtle effects that somewhat complicate the interpretation of charge state measurements for multi-stage species like iron (Owocki 1982), but, for the sake of brevity, we shall not discuss these effects here.

For other reasonable expansion models, the freezing radius of a given exchange does not vary by more than $\sim 0.5 R_\odot$ from that in this typical spherical expansion model. For example, for a coronal hole model with the same particle flux as above, but with a flow-tube area that increases from the sun to 1 a.u. by a factor 7 more than in spherical expansion, we find for the oxygen balance $n_f = 5 \times 10^7 cm^{-3}$, which because of the much lower coronal density (see e.g. Munro and Jackson 1977) gives $r_f = 1 R_\odot$. However, because the pressure measured (e.g. Withbroe 1977) at the coronal base is $nT > 10^{14} cm^{-3} {}^oK$, we find that the oxygen

ionization state must still freeze at coronal temperatures $T=10^{6}{}^{o}K$. This implies that all ionization exchanges as fast or faster than oxygen always freeze at or above the coronal base, and so the measured interplanetary charge state is sensitive only to coronal conditions, and not to conditions in the underlying chromosphere and transition region.

Having established this basis for understanding the ionization state freezing in simple coronal ion outflows, we shall now examine in the following sections the effect of relaxing some of the simplifying assumptions made above.

3. Effect of Unequal Ion Flow Speeds

We first examine how the above freezing-in theory is altered when the flow speeds u_i of different charge-stages of a given species are not all equal. Such unequal outflow of heavy ions from the corona cannot be precluded on either observational or theoretical grounds because only a few measurements of coronal ion flow speeds exist (Cushman and Rense 1976; Rottman et al. 1981; Withbroe et al. 1982), and because the mechanism by which the heavy ions are accelerated in the corona is not well-understood. The usual coronal pressure-gradient force is insufficient to drive these heavy ions outward against their stronger confinement by solar gravity (Geiss et al. 1970), and yet interplanetary measurements indicate substantial fluxes of all heavy ions at a common speed equal to or slightly greater than the solar wind proton speed (Ogilvie et al. 1980; Schmidt et al. 1980). This implies that unknown, additional acceleration mechanisms must exist for heavy ions in the corona. Examples of mechanisms which have been considered are coulomb friction from the protons (Geiss et al. 1970), interaction with MHD waves (Dusenbery and Hollweg 1981), and enhanced pressure-gradient forces resulting from preferential ion heating (Ryan and Axford 1975). As with most additional acceleration mechanisms that one can imagine, the forces for all of these vary with ion charge, and this suggests that the various charge-stages of a given ion species may not accelerate and flow uniformly in the corona.

The major consequence of such unequal ion flow speeds for the freezing of the solar wind ionization state can be understood from the discussion in section 2. Recall from there that, although the ionization equilibrium conditions (2) at the coronal base determine the relative number of various ion charge-stages, the freezing-in condition (3) for the solar wind fixes the relative flux of these charge stages. With unequal coronal flow speeds, an interplanetary measurement of the frozen-in values of the relative ion fluxes can therefore no longer be used to infer directly the relative ion abundances, and hence the electron temperature, in the coronal freezing-in region. If the ion flow speeds in the corona are known, this mismatch between abundances fixed by ionization equilibrium and fluxes fixed by the freezing condition can be readily resolved (see Owocki et al. 1983). One need only correct the measured frozen-in flux ratios by the ratio of the ion flow speeds at the freezing radius, r_f, to obtain the appropriate abundance ratios, from which the electron temperature at r_f can be estimated using equation (2).

This simple result makes it easy to estimate the error in inferred electron temperature that would result from ignoring the effects of ion flow speeds that differ in the corona by known ratios. The sense of the errors are such that the temperature inferred by traditional interpretation of the interplanetary ionization state will overestimate (underestimate) the actual coronal electron temperature if higher ion charge stages flow systematically faster (slower) than lower stages at the coronal freezing radius. For a given flow-speed-ratio, the magnitude of these errors will vary depending on how sharply the ionization/recombination rate ratio $R_{i+1}(T_e)/C_i(T_e)$ varies with electron temperature T_e. For balances among dominant coronal oxygen charge-stages, a coronal flow-speed ratio of 5 results in an error in inferred temperature of 0.5×10^6 ^oK. Iron balances show greater sensitivity, with such a temperature error of 0.5×10^6 ^oK resulting from only a factor of 2 difference between neighboring iron charge-stage flow speeds.

4. Effect of a Non-Maxwellian Electron Velocity Distribution

We next examine how the relationship between coronal degree of ionization and coronal electron temperature is altered by a local electron velocity distribution that is not Maxwellian. Direct samplings of the electron velocity distributions in the solar wind have shown that, while the low-energy distribution "cores" can be well-fit by a Maxwellian, the high-energy "tails" of these distributions are best fit by a power law in energy, and so are enhanced relative to a Maxwellian of the same mean particle energy (Montgomery et al. 1968, 1972; Feldman et al 1975; Rosenbauer et al. 1976; Ogilvie and Scudder 1978). Scudder and Olbert (1979a,b) have argued that this observed enhancement in the high-energy tail of the interplanetary electron velocity distribution arises because of the decline of the coulomb collision cross-section at high electron energies. This allows higher-energy coronal electrons to travel with few collisions upward from the high-density corona into the low-density solar wind, where they enhance the tail of the local velocity distribution. According to this theory of global transport for high-energy electrons, the strong density gradient throughout the solar corona should also result in locally enhanced high-energy tails in the electron velocity distribution of the corona itself (Olbert 1983).

Recently, Owocki and Scudder (1983) have examined how the coronal ionization balances $O^{+6} <-> O^{+7}$ and $Fe^{+11} <-> Fe^{+12}$ depend on the shape of the electron distribution (i.e. on the magnitude of the high-energy tail enhancement), as well as on the electron temperature. They employ a parameterized non-Maxwellian distribution, the "kappa distribution" (Olbert 1967, 1969), for which the relative deviation of the distribution from a Maxwellian shape can be readily varied through changes in the free parameter, κ. As with the distributions observed in the solar wind and postulated for the solar corona, this kappa distribution closely approximates a Maxwellian in the low-energy "core", but varies as a power law in its enhanced high-energy tail (see figure 2). Although the lower level of each of the studied exchanges is the most abundant stage in an

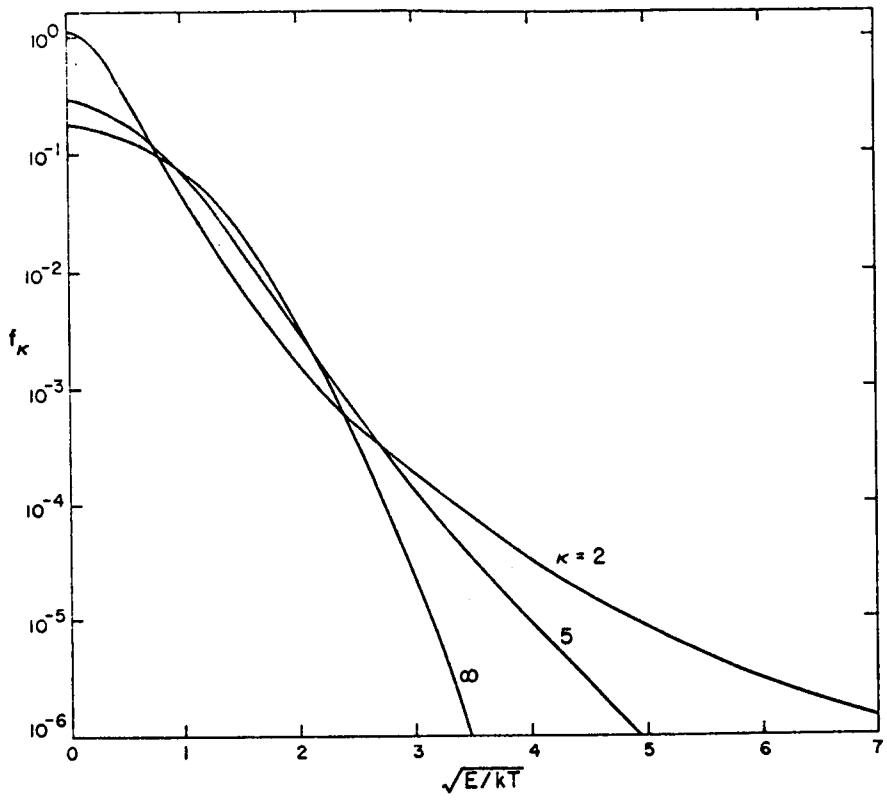

Figure 2: Kappa electron distribution function f vs. the square root of the electron kinetic energy over thermal energy, $\sqrt{E/kT}$, for kappa distributions with $\kappa = 2$ and 5 and a Maxwellian ($\kappa = \infty$). The temperature T is assumed to be equal for all three distributions.

equilibrium balance at a typical coronal temperature of 1.5×10^6 °K (Allen and Dupree 1969; Jordan 1969, 1970), the oxygen ionization threshold energy is actually more than twice that of iron (i.e. $\chi(O^{+6}) = 739$ eV vs. $\chi(Fe^{+11}) = 331$ eV). An enhanced high-energy tail in the coronal electron distribution therefore has a greater effect on the oxygen ionization balance.

Figure 3 graphically illustrates for the oxygen ionization exchange $O^{+6} \longleftrightarrow O^{+7}$ the relative sensitivity of collisional ionization rate and radiative recombination rate to the presence of an enhanced tail on the electron distribution function. In each of the upper, central, and lower two boxes of figure 3, the shaded areas are proportional respectively to the ionization rate, recombination rate, or mean electron energy (i.e. electron temperature) in either a Maxwellian distribution (i.e. with $\kappa = \infty$; left boxes) or in a kappa distribution with $\kappa = 3$ (right boxes). The two distributions have been adjusted to have equal

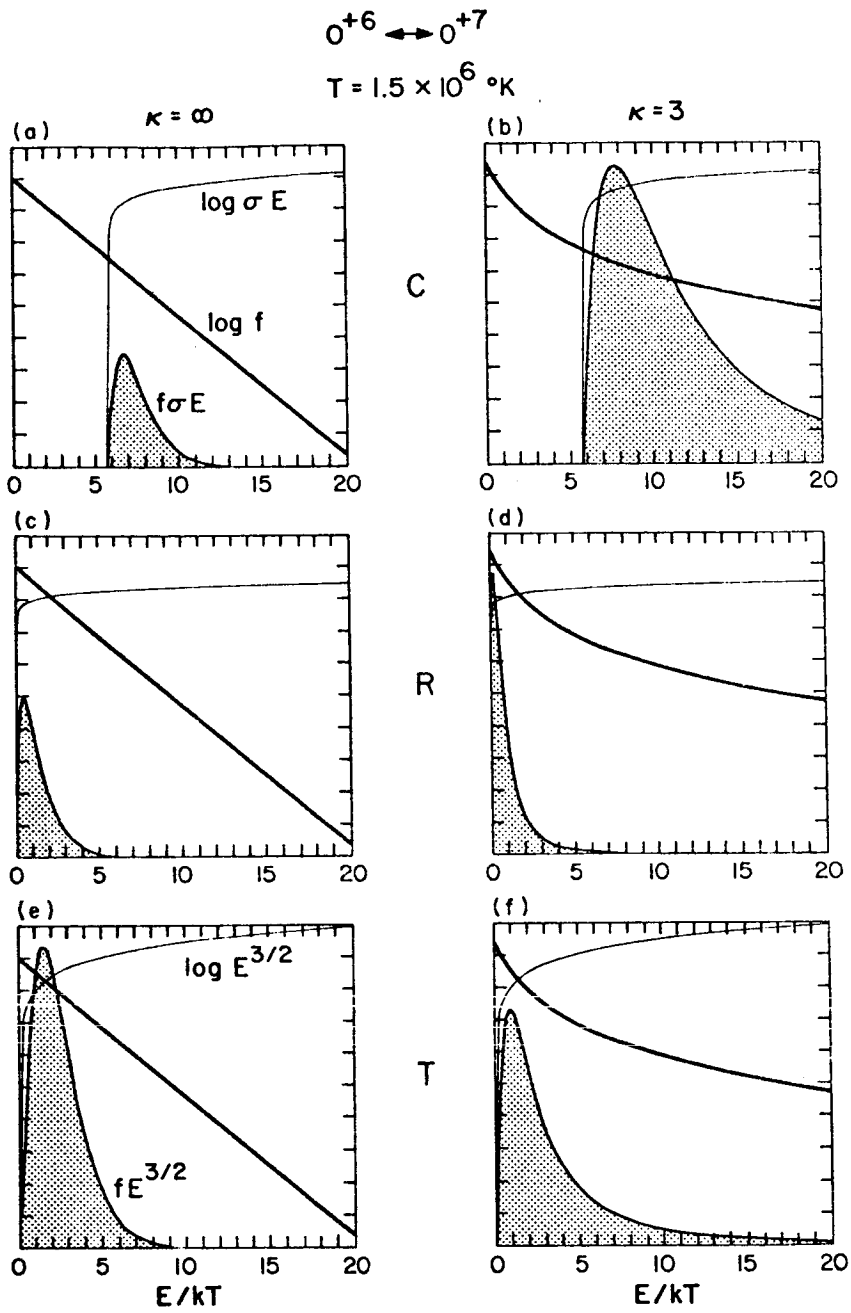

Figure 3: Comparison of collisional ionization (C) and radiative recombination (R), for the oxygen ionization balance $O^{+6} \leftrightarrow O^{+7}$ in a Maxwellian ($\kappa=\infty$; left boxes) and in a kappa distribution ($\kappa=3$; right boxes). In the upper four boxes (a-d), the heavy and light solid lines show respectively the logarithmic variations of the distribution function f and the cross section times energy E, while the linear variation of the relevant rate integrand $f\sigma E$ outlines the shaded areas, which are thus proportional to the relevant rates $\langle\sigma v\rangle$. In the lower two boxes (e,f) the cross section is replaced by the square root of the energy, $\sqrt{E}$, and the equality of the shaded areas, now proportional to the mean kinetic energy $\langle E\rangle=3kT/2$, shows that the two distributions have the same kinetic temperature ($T=1.5\times10^6$ °K).

temperatures $T=1.5\times10^6$ °K, as can be seen from the equality of the shaded areas in the lower two boxes (cf. figures 3e,f). Comparison of the shaded areas in the central two boxes (cf. figures 3c,d), which are proportional to the respective radiative recombination rates, shows that in the kappa distribution recombination occurs at a slightly higher rate, and with electrons of slightly lower energy, than in the Maxwellian. By contrast, the impact ionization rates are significantly increased by the enhanced high-energy tail of the kappa distribution (cf. figures 3a and 3b). The net result (see equation (2)) is that a kappa distribution can support a much higher degree of oxygen ionization than a Maxwellian with the same temperature. Qualitatively, we therefore expect that interpretations of the oxygen charge state based on the assumption of a Maxwellian will systematically overestimate the electron temperature if the electron distribution actually has an enhanced high-energy component.

Because it is the ionization ratio, n_i/n_{i+1} ($=R_{i+1}/C_i$ in ionization equilibrium; eqn. (2)), and not the individual rates R_i or C_i, that can be inferred from direct sampling of the frozen-in ratio in the solar wind, it is important to establish quantitatively the range in electron distribution function properties that are compatible with a given ratio in ionization equilibrium. In figures 4a and 4b contours of the iron (Fe^{+11}/Fe^{+12}) and oxygen (O^{+6}/O^{+7}) equilibrium ionization ratios are plotted for electron velocity distributions that range from Maxwellian ($\kappa=\infty$) to extremely non-Maxwellian ($\kappa=2$) and that range in temperature from $T=1\times10^6$ °K to 3×10^6 °K. The path along any contour denotes the appropriate combinations of T and κ that are consistent with an ionization ratio measurement of the value that labels the contour. For example, note from figure 4b that an oxygen ionization ratio $n_{+6}/n_{+7}=1$ is consistent with a Maxwellian distribution with $T=2\times10^6$ °K and $\kappa=\infty$, but it is also consistent with a kappa distribution with $T=1.3\times10^6$ °K and $\kappa=2.5$. If the latter parameter set better represented the electron distribution function in the solar corona, then an oxygen ionization ratio measurement, if interpreted on the basis of the traditional assumption of a Maxwellian electron distribution, would lead to an electron temperature overestimate of about 0.7×10^6 °K.

A temperature overestimate of this kind will occur whenever the contours in figure 4 slope downward as one moves away from the Maxwellian limit denoted by the left ordinate. Conversely, an upward slope implies a temperature underestimate when one incorrectly assumes a Maxwellian, while a zero (or small) slope implies that the equilibrium ionization ratio is relatively insensitive to assumptions about the form of the distribution. The oxygen contours generally slope downward; the iron contours either have zero or upward slopes (cf. figures 4a and 4b). Hence, in contrast to the temperature overestimates typical for oxygen, the iron charge state ratios are either insensitive to the form of the distribution or yield temperature underestimates when a Maxwellian is incorrectly assumed (viz. the contour labeled "1" in figure 4a). Even the oxygen contours do not, however, continue to slope downward for extreme departures from a Maxwellian; rather they reach a minimum for $\kappa=3$, so that the magnitude of temperature overestimates based on measured oxygen ionization ratios is limited to

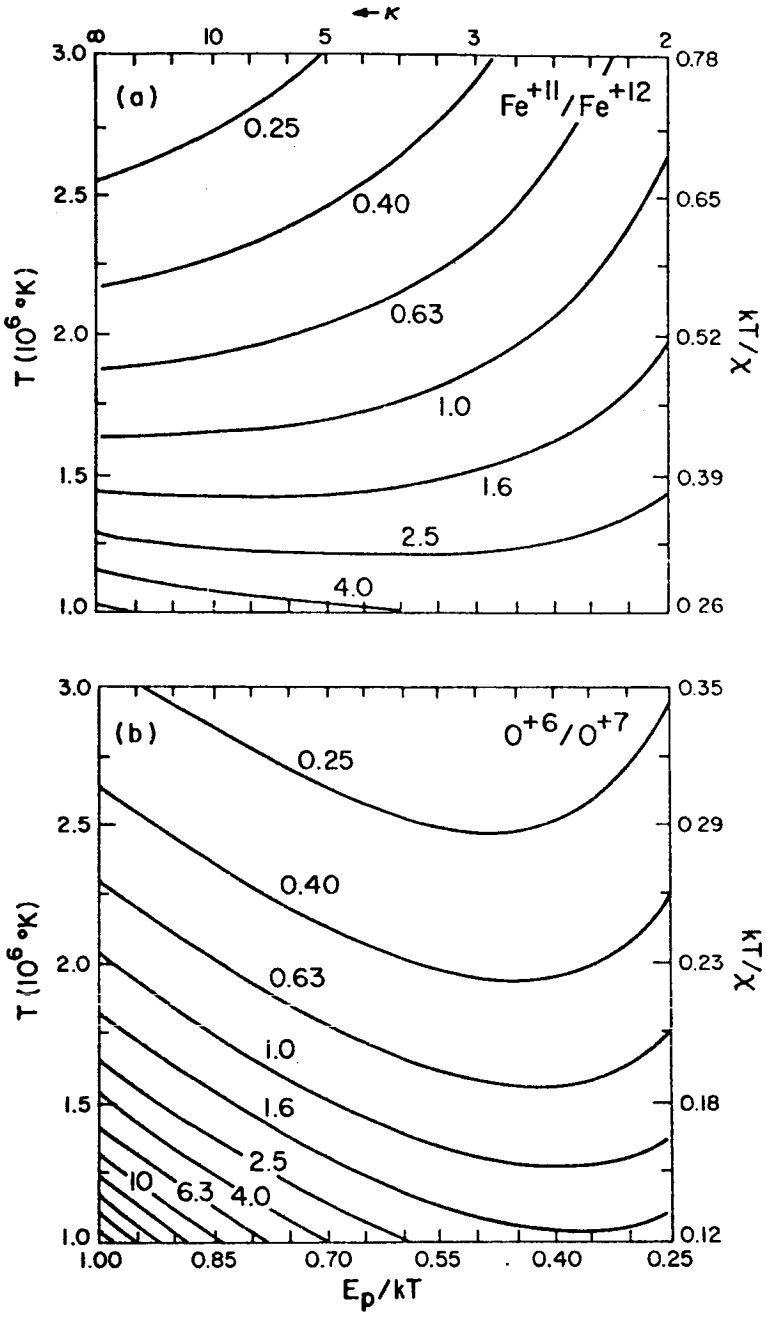

Figure 4: a. Contours of iron ionization ratio Fe^{+11}/Fe^{+12} as a function of kinetic temperature T and of core to total energy ratio $E_p/kT=(\kappa-3/2)/$. The right ordinate is labeled with the ratio, kT/χ, of thermal energy to ionization threshold energy, the upper abscissa is labeled with the value of the distribution parameter κ , and each contour is labeled with the appropriate ionization ratio.

b. Same as a, except for the oxygen ratio O^{+6}/O^{+7}.

$<0.75 \times 10^6$ °K. This upturn in equilibrium ionization ratio contours for extreme non-Maxwellian distributions stems mostly from the recombination rate increase associated with the enhancement in the low-energy energy core of the distribution (see figure 2; also figures 3c,d).

We thus see that, relative to a Maxwellian of the same mean electron energy, the degree of ionization allowed by a non-Maxwellian distribution with an enhanced high-energy tail is either unchanged or slightly decreased for iron, but can be substantially increased for oxygen. As a result, the coronal electron temperature inferred from an interplanetary measurement of the frozen-in oxygen ionization ratio, O^{+6}/O^{+7}, could overestimate the actual coronal electron temperature by as much as 0.75×10^6 °K. The unexpectedly high degree of oxygen ionization measured in the high-speed solar wind (Ogilvie and Vogt 1980) may therefore result from an enhanced tail in the electron velocity distribution in the coronal source regions of such high-speed wind, rather than from an enhanced coronal electron temperature.

5. Effect of a Time-Variations Associated with a Coronal Shock Wave

Finally, we examine how the freezing-in of the solar wind ionization state is affected by rapid time variations at the base of the coronal expansion. Observations indicate that activity in the solar photosphere and chromosphere can have an outward-propagating effect, inducing sudden changes in the solar corona and the solar wind. For example, white-light coronagraphs have detected upward-moving coronal density variations, often called "coronal transients", in association with flares and/or eruptive prominences (MacQueen 1980), and measurements with interplanetary spacecraft indicate that some 50% of the energy in large flare events is propagated through the corona and into the solar wind (Hundhausen 1972). These coronal time-variations can strongly influence the ionization state of interplanetary gas observed in association with solar activity (Bame et al. 1979; Fenimore 1980), and interpretation of interplanetary charge-state measurements should therefore take into account the effect of such intrinsic variability. We shall investigate such effects below for a relatively simple picture of the time-dependent coronal flow, based on a model of a self-similar shock wave propagating through the corona.

For simplicity we assume in this model that the electron distribution is Maxwellian, that the coronal outflow is spherically-symmetric, and that all heavy-ion charge-stages flow everywhere at the proton speed ($u_i = u$ for all i). From the last assumption, we conclude that there is no net flux of ions into or out of a fluid parcel that flows at the speed u, and so the ionization state of each parcel is independent of conditions in neighboring parcels. This means that equations (1) can be simplified so that all ionization state changes can be described in terms of a total derivative with respect to a Lagrangian coordinate r_L,

$$\frac{Dn_i}{Dr_L} \equiv \frac{1}{u}\frac{\partial n_i}{\partial t} + \frac{\partial n_i}{\partial r} = \frac{n_e}{u}\left(n_{i-1}C_{i-1} - n_i(C_i+R_i) + n_{i+1}R_{i+1}\right) \quad . \tag{5}$$

Given the flow speed u, electron density n_e, and electron temperature T_e as functions of the Lagrangian coordinate r_L, eqn. (5) can be numerically integrated for each fluid parcel to obtain the ionization state evolution in r_L. Reconstruction of the ionization state time variation at a fixed Eulerian space coordinate r (e.g. at r= 1 a.u.) then follows readily from the known ionization state of many fluid parcels flowing past the fixed coordinate at the known speed u.

To investigate the ionization effects of coronal shocks, Owocki and Hundhausen (1983) (see also Owocki 1982) use a kinematic description of strong coronal shocks in which they obtain, as required for calculation of the ionization state, the Lagrangian evolution of velocity, density, and temperature. We consider here only the special case in which the shock speed V is constant and the post-shock flow is neither compressive nor expansive. In this simple shock model, each fluid parcel experiences a sudden jump in velocity, density, and

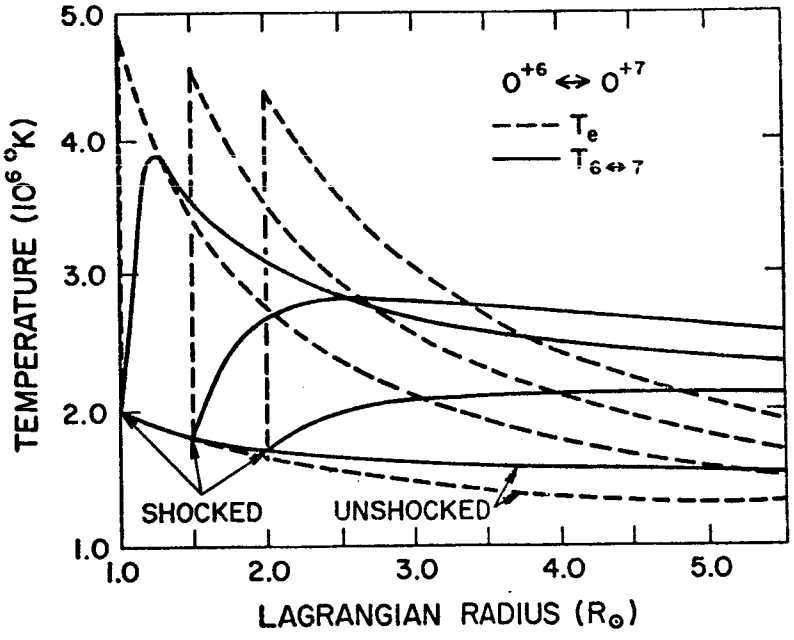

Figure 5: Lagrangian evolution of oxygen ionization ratio temperature $T_{6<\rightarrow 7}$ in ambient unshocked wind and in fluid parcels shocked at R_1=1, and 1.5, and $2R_\odot$ in non-compressive, constant-speed shock models with various shock speeds V. Dashed curves denote evolution of electron temperature T_e.

temperature at its shock location $r_L=R_1$, after which the velocity is constant at $u=3V/4$, the density declines with the outward spherical expansion as $n_e=4n_a(R_1)(r_L/R_1)^{-2}$, ($n_a$ is the density in the ambient, unshocked flow) and the temperature excess declines adiabatically as $T\sim r_L^{-4/3}$.

Figure 5 plots for this shock model the evolution of electron temperature (dashed curves) and oxygen ionization ratio temperature $T_{6<\rightarrow>7}$ (solid curves) vs. Lagrangian radius r_L for the ambient, unshocked flow and for three fluid parcels that are shocked respectively at $R_1=1$, 1.5, and $2R_\odot$. (The ionization ratio temperature is defined as the electron temperature that, in ionization equilibrium, would yield a given abundance ratio of, e.g., O^{+6} vs. O^{+7}; see Owocki 1982). Note that fluid parcels shocked at greater radii show progressively weaker ionization ratio temperature responses to the shock, but the net gain in the asymptotic, frozen-in, ratio temperature is highest for the parcel shocked at the intermediate height $R_1=1.5R_\odot$. The parcel shocked at $R_1=1R_\odot$ initially shows a stronger jump in ionization ratio temperature, but it then continues to follow the local electron temperature as the parcel adiabatically cools. It thus freezes at a ratio temperature (1.8×10^6 °K) enhanced only slightly above the value for the ambient flow (1.6×10^6 °K). On the other hand, the ionization state in the parcel with $R_1=2R_\odot$, being nearly frozen-in when shocked, does not follow this adiabatic cooling; but neither is its initial jump in ratio temperature very great, and so its frozen-in ratio temperature (1.8×10^6 °K) is also only slightly enhanced above that of the ambient flow. The parcel shocked at $R_1=1.5R_\odot$ is intermediate between the frozen-in, small-jump case and the equilibrium, adiabatic-cooling case, and thus shows the greatest frozen-in ratio temperature (2.1×10^6 °K).

Figure 6 shows the temporal variation of frozen-in oxygen ionization ratio temperature $T_{6<\rightarrow>7}(r=1\text{a.u.})$ that results at 1 a.u. from coronal shocks with various shock speeds V. The abscissa gives the time t for passage of a coronally-shocked fluid parcel relative to the time for passage of a parcel shocked at $R_1=10R_\odot$. All such fluid parcels trail by several hours the interplanetary passage of the shock itself. The dot that terminates each curve represents the time for passage of the parcel shocked at the coronal base; i.e. with $R_1=1R_\odot$. Because we have not included here any model of the driver gas, these shock calculations give no information on the ionization state after this time. (For flare-associated disturbances, this driver gas may be flare-heated plasma that itself has a very high degree of ionization.) The calculations do suggest, however, that a few hours after the passage of a flare-associated interplanetary shock, and shortly before arrival of the flare-heated driver gas that caused the shock, a spacecraft at r= 1 a.u. should observe a peak in ionization temperature (e.g. for oxygen) lasting for a few time ten minutes. However, this would require time resolution that is somewhat beyond the capability of current detectors.

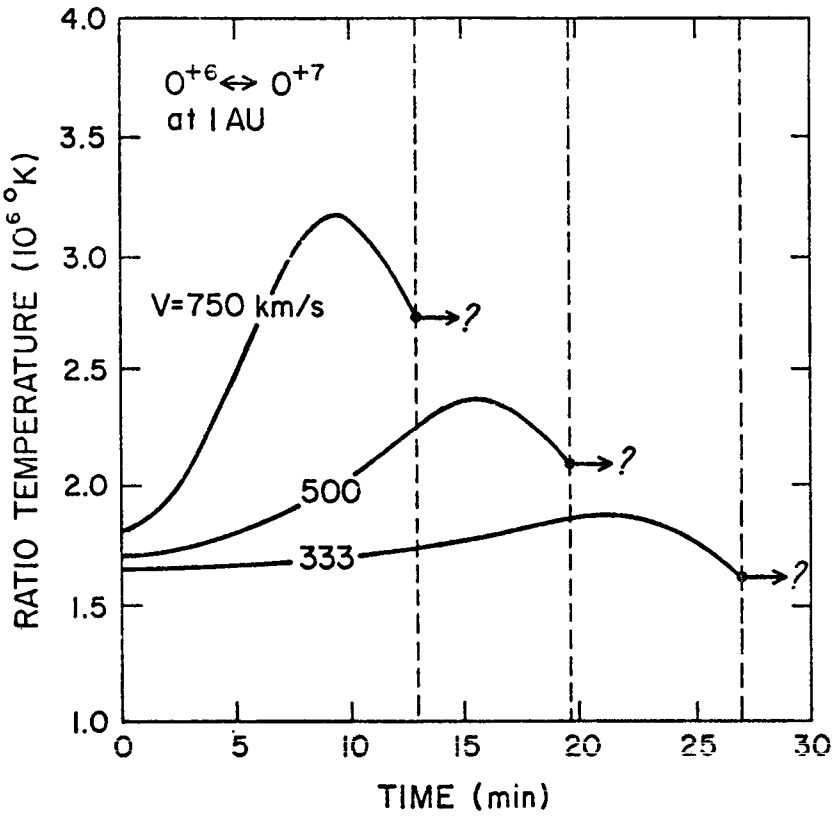

Figure 6: Interplanetary oxygen ionization ratio temperature $T_{6<->7}$ vs. time t since passage of parcel shocked at $R_1=10R_\odot$, for non-compressive, constant-speed shock models with various shock speeds V.

6. Summary

In this paper, we have examined the freezing of the solar wind ionization state for various conditions in the expanding solar corona. We first reviewed this freezing theory for spherically-symmetric, steady-state coronal expansion in which the coronal electron velocity distribution is Maxwellian and the coronal flow speeds of the various charge-stages of heavy ion species are all equal to the proton speed. We found in this case that the relative flux of heavy ion charge-stages could be straightforwardly interpreted to yield the electron

temperature at a discrete coronal freezing radius. We next examined the case in which the coronal flow speeds of the various charge-stages of a given heavy ion species were not equal. In this case frozen ion flux ratios had to be first scaled by the ratios of ion flow speeds at the freezing radius to obtain an accurate estimate of coronal charge-stage abundance ratios, from which the coronal electron temperature could then be inferred. Without this correction, the inferred temperature was found to overestimate (underestimate) the actual coronal electron temperature when higher (lower) charge-stages flowed faster at the freezing radius.

We also examined the coronal ionization balances $O^{+6} <-> O^{+7}$ and $Fe^{+11} <-> Fe^{+12}$ when the high-energy tail of the coronal electron velocity distribution was enhanced relative to a Maxwellian distribution. We found that the degree of oxygen ionization in such a distribution was greatly increased relative to a Maxwellian with the same mean energy (ie. same temperature), but the degree of ionization of iron was relatively unaffected. The greater sensitivity of the oxygen ionization balance to the enhancement in the high-energy tail of the electron distribution was attributed to the higher oxygen ionization potential. We find, in particular, that temperatures inferred from oxygen charge-stage ratios can overestimate the true electron temperature by as much as 0.75×10^6 ^oK if the electron distribution is incorrectly assumed to be strictly Maxwellian.

Finally, we examined the ionization state freezing in the time-varying conditions associated with a coronal disturbance, e.g. passage of a strong coronal shock-wave. If the various charge-stages in such a flow have equal bulk flow speeds, then the flow ionization state can be conveniently studied using a Lagrangian approach of following the evolution of individual fluid parcels. For a strong coronal shock-wave, we find that only parcels shocked near or below the ambient-flow freezing radius show a marked ionization state response to the shock. As a result, the time-variation of the charge state in the resulting interplanetary disturbance is limited to a few times ten minutes, which corresponds to the time required for the shock to transit the low corona.

In summary, we find that various coronal effects, such as unequal ion flow speeds, a non-Maxwellian electron distribution, or intrinsic time-variations, can alter the usual freezing picture of the solar wind ionization state, but there remains nonetheless a close association between interplanetary charge state and coronal electron temperature. We therefore encourage the careful interpretation of interplanetary charge state measurements to infer the physical state, particularly electron temperature, in coronal outflows with a variety of conditions.

Acknowledgements: The results reported here are based on thesis research done with support of a graduate research assistantship at the High Altitude Observatory of the National Center for Atmospheric Research. This paper was prepared with support of the Langley-Abbott program of the Smithsonian Institution and NASA grant NAGW-249.

References

Allen, J.W. and A.K. Dupree, Calculations of ionization equilibria for oxygen, neon, silicon, and iron, Ap. J., 155, 27, 1969.

Bame, S.J., J.R. Asbridge, W.C. Feldman, and P.D. Kearney, The quiet corona: temperature and temperature gradient, Solar Phys., 35, 137, 1974.

Bame, S.J., J.R. Asbridge, W.C. Feldman, E.E. Fenimore, and J.T. Gosling, Solar wind heavy ions from flare-heated coronal plasma, Solar Phys., 62, 179, 1979.

Billings, D.E., A Guide to the Solar Corona, Academic Press, New York and London, 1966.

Burgess, A., A general formula for the estimation of dielectronic recombination coefficients in low-density plasmas, Ap. J. Lett., 141, 1588, 1965.

Cushman, G.W. and W.A. Rense, Evidence of outflow of plasma in a coronal hole, Ap. J. Lett., 207, L61, 1976.

Dusenbery, P.B. and J.V. Hollweg, Ion-cyclotron heating and acceleration of solar wind minor ions, J. Geophys. Res., 86, 153, 1981.

Feldman, W.C., J.R. Asbridge, S.J. Bame, M.D. Montgomery, and S.P. Gary, J. Geophys. Res., 80, 4181, 1975.

Feldman, W.C., Asbridge, J.R., Bame, S.J. and Gosling, J.T. 1977, in The Solar Output and Its Variation, O.R. White, ed., (Boulder: Univ. of Colorado Press).

Fenimore, E.E., Solar wind flows associated with hot heavy ions, Ap. J. 235, 245, 1980.

Geiss, J.P., P. Hirt, and H. Leutwyler, On acceleration and motion of ions in corona and solar wind, Solar Phys., 12, 458, 1970.

Hundhausen, A.J., Coronal Expansion and Solar Wind, Spring-Verlag, New York, Heidelberg, and Berlin, 1972.

Hundhausen, A.J., H.E. Gilbert, and S.J. Bame, The state of oxygen ionization in the solar wind, Ap. J. Lett., 152, L3, 1968a.

Hundhausen, A.J., H.E. Gilbert, and S.J. Bame, Ionization state of the interplanetary plasma, J. Geophys. Res., 73, 5485, 1968b.

Jordan, C., The ionization equilibrium of elements between carbon and nickel, M.N.R.A.S., 142, 501, 1969.

Jordan, C., Ionization equilibria for high ions of Fe and Ni, M.N.R.A.S. 148, 17, 1970.

Lotz, W., Electron impact ionization cross-sections and ionization rate coefficients for atoms and ions, Ap. J. Suppl., 14, 207, 1967.

MacQueen, R.M, Coronal transients: a summary, Phil. Trans. R. Soc. Lond., 297, 605, 1980.

Montgomery, M.D., Thermal energy transport in the solar wind, in Cosmic Plasma Physics, Shindler, ed., Plenum Press, New York, p. 61, 1972.

Montgomery, M.D., Bame, S.J., and Hundhausen, A.J., Solar wind electrons: Vela 4 measurements, 73, 4999, 1968.

Munro, R.H. and B.V. Jackson, Physical properties of a polar coronal hole from 2 to 5 $R_\odot$, Ap. J., 213, 874, 1977.

Newkirk, G., Structure of the solar corona, Ann. Rev. Astron. Astrophys., 5, 213, 1968.

Ogilvie, K.W. and J.D. Scudder, The radial gradients and collisionless properties of solar wind electrons, J. Geophys. Res., 83, 3776, 1978.

Ogilvie, K.W. and C. Vogt, Variations of the average 'freezing-in' temperature of oxygen ions with solar wind speed, Geophys. Res. Lett., 7, 577, 1980.

Ogilvie, K.W., P. Bochsler, J. Geiss, and M.A. Coplan, Observations of the velocity distribution of solar wind ions, J. Geophys. Res., 85, 6069, 1980.

Olbert, S., AGU Abstracts, Washington, 1967.

Olbert, S., in Physics of Magnetospheres, R.C. Carovillano, J.F. McClay, H.R. Radoski, eds., 641, D.Reidel, Dordrecht, Holland, 1969.

Olbert, S., this volume, 1983.

Owocki, S.P., The Ionization State of the Solar Wind, Ph. D. Thesis, Univ. of Colo. and National Center for Atmospheric Research, NCAR CT-66, Boulder, 1982.

Owocki, S.P., T.E. Holzer, and A.J. Hundhausen, The solar wind ionization state as a coronal temperature diagnostic, submitted to Ap. J., 1983.

Owocki, S.P. and A.J. Hundhausen, A.J., The effect of a strong coronal shock on the solar wind ionization state, submitted to Ap. J., 1983.

Owocki, S.P. and J.D. Scudder, The effect of a non-Maxwellian electron distribution on oxygen and iron ionization balances in the solar corona, Ap. J., in press, 1983.

Rosenbauer, H., H. Miggenreider, M. Montgomery, and R. Schwenn, in Physics of Solar and Planetary Environments, D. Williams, ed., 319, AGU, Washington, 1976.

Rottman, G.J., Orrall, F.Q., and Klimchuk, J.A., Measurement of systematic outflow (?) from the solar transition region underlying a coronal hole, 1981. Astrophys. J. Lett., 247, L135.

Ryan, J.M. and W.I. Axford, The behaviour of minor species in the solar wind, J. Geophys., 41, 221, 1975.

Saito, K., A non-spherical axisymmetric model of the solar K-corona of the minimum type, Ann. Tokyo Astron. Observ. - Ser. 2, 12, 53, 1970.

Schmidt, W.K.H., H. Rosenbauer, E.G. Shelly, and J. Geiss, On the temperature and speed of He^{++} and O^{6+} ions in the solar wind, Geophys. Res. Lett., 7, 697, 1980.

Scudder, J.D. and S. Olbert, A theory of local and global processes which affect solar wind electrons: I. The origin of typical 1 AU velocity distribution functions, J. Geophys. Res., 84, 2755, 1979a.

Scudder, J.D. and S. Olbert, A theory of local and global processes which affect solar wind electrons: II. Experimental support, J. Geophys. Res., 84, 6603, 1979b.

Seaton, M.J., The spectrum of the solar corona, Planet. Sp. Sci., 12, 55, 1964.

Tucker, W.H. and Gould, R.J., Radiation from a low-density plasma at 10^{6o}K to 10^{8o}K, Ap. J., 144, 244, 1966.

Withbroe, G.L., J.L. Kohl, H. Weiser, G. Noci, and R.H. Munro, Analysis of coronal HI Lyman alpha measurements from a rocket flight on 1979 April 13, Ap. J., 254, 361, 1982.